Table of Contents

Appendix Figures S1-S23 & Figure legends

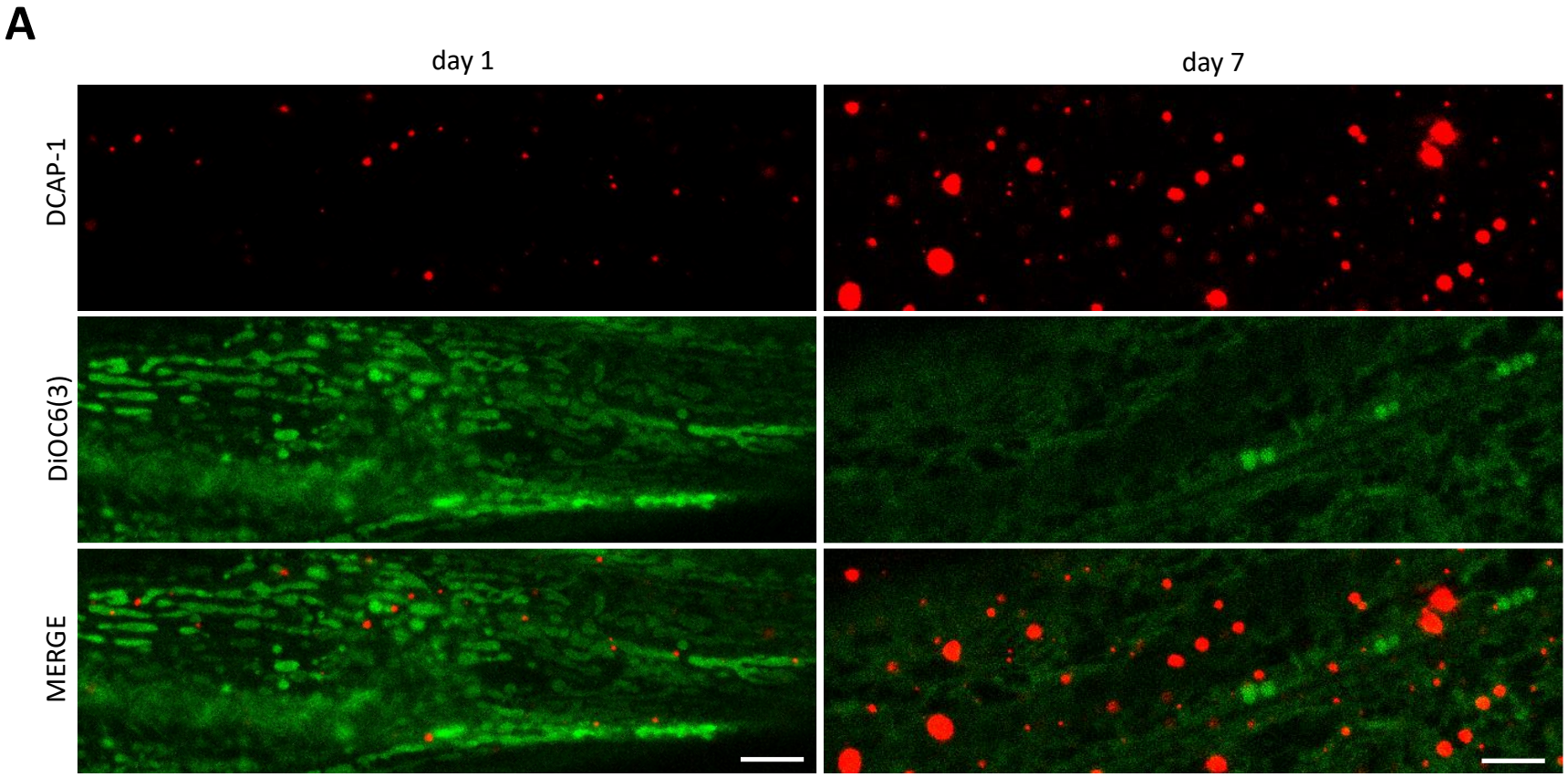

Appendix Fig S1

Appendix Figure S1 - Association of DCAP-1-foci with mitochondria is age-dependent. A Representative images showing the localization of DCAP-1-foci relative to mitochondria in young versus older animals (red: DCAP-1, green: DiOC6(3), a mitochondrial-specific dye; n=2 independent experiments). **B** Quantification of the distances between DCAP-1-foci and mitochondria in young versus older animals (n=2 independent experiments with at least 40 animals/experiment; **P<0.01; two-tailed unpaired t-test).

Data information: Scale bars, 10μm. Images were acquired using a X63 objective lens. Error bars denote SEM.

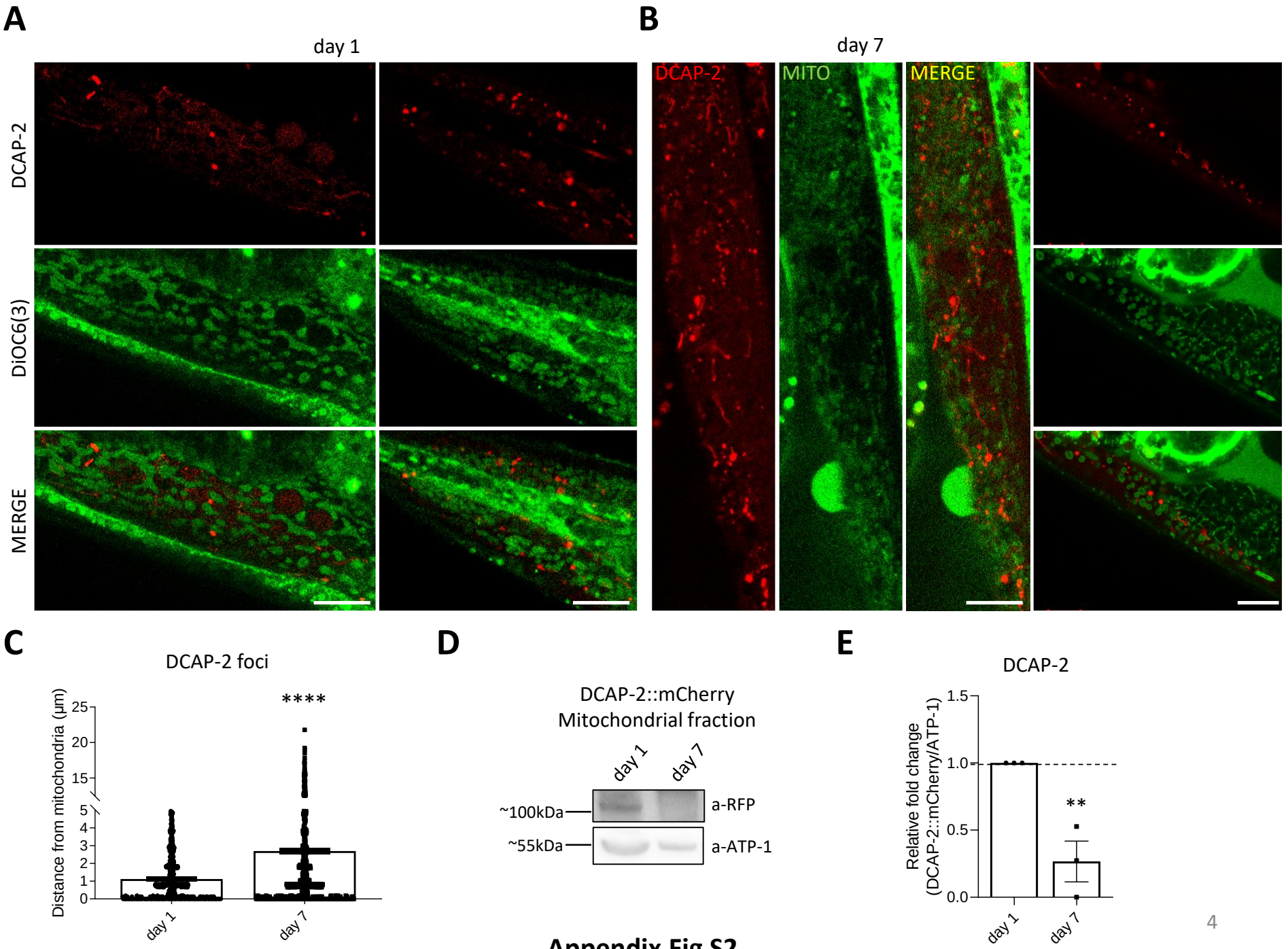

Appendix Fig S2

Appendix Figure S2 - Association of DCAP-2-foci with mitochondria is age-dependent. Representative images showing the localization of DCAP-2-foci relative to mitochondria in **A**, young versus **B**, old animals (red: DCAP-2, green: DiOC6(3), a mitochondrial-specific dye; n=2 independent experiments). **C**, Quantification of the distances between DCAP-2-foci and mitochondria in young versus old animals (n=2 independent experiments with at least 40 animals/experiment; ****P<0.0001; two-tailed unpaired t-test). **D**, Representative image from Immunoblot analysis showing that DCAP-2 is less associated with mitochondria during ageing and **E**, Respective quantification showing DCAP-2 levels normalized to ATP-1 (n=3 independent experiments, **P<0.01; two-tailed unpaired t-test).

Data information: Scale bars, 10μm. Images were acquired using a X63 objective lens. Error bars denote SEM.

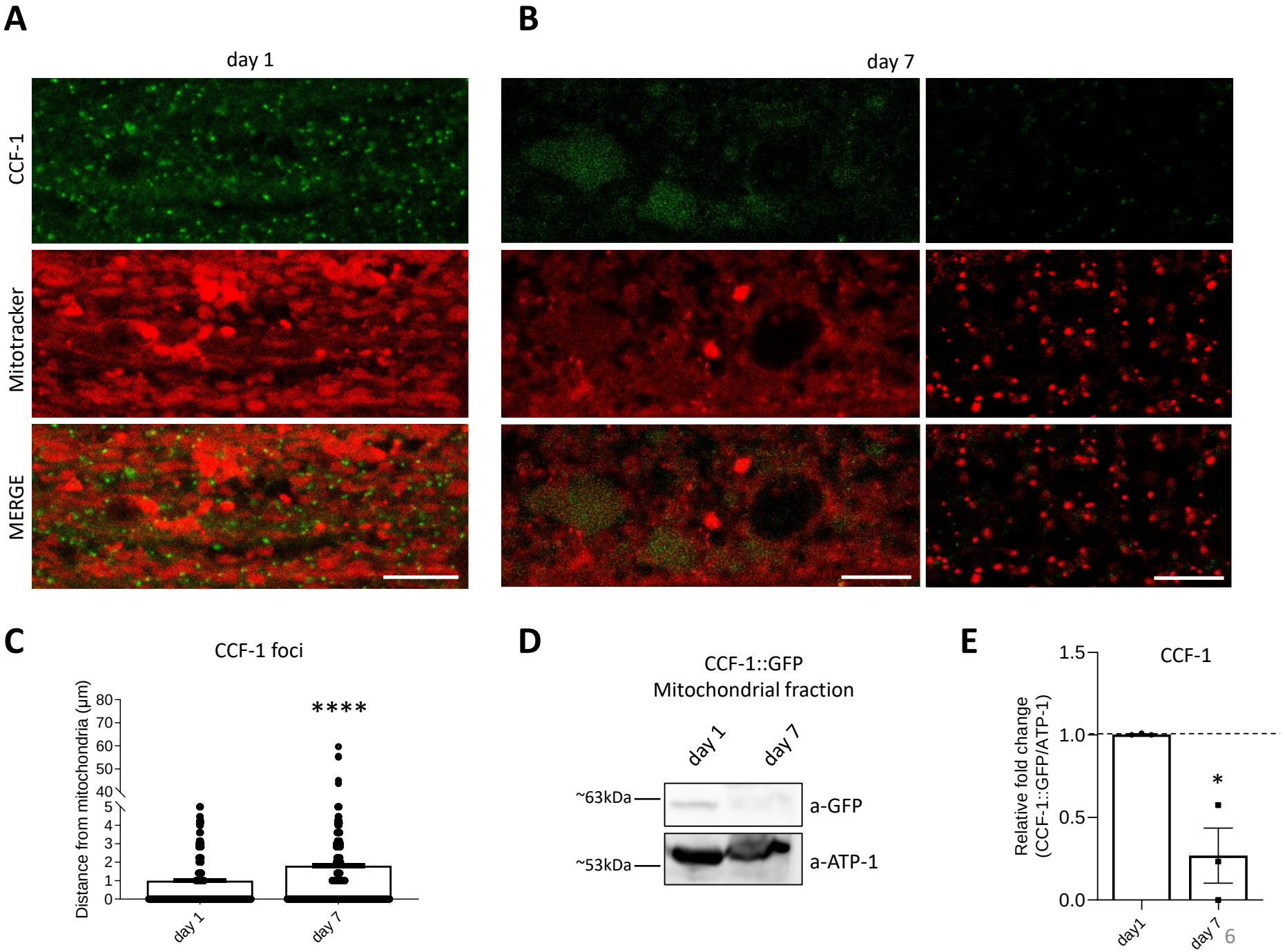

Appendix Fig S3

Appendix Figure S3 - Association of CCF-1-foci with mitochondria is age-dependent. Representative images showing the localization of CCF-1-foci relative to mitochondria in **A**, young (1-day-old) versus **B**, old (7-day-old) animals (image in control is reused in Fig EV2E as conditions indicated in Appendix Fig S3A & Fig EV2E are part of the same experimental setup) (green: CCF-1, red: Mitotracker Deep Red FM, a mitochondrial-specific dye; n=2 independent experiments). **C**, Quantification of the distances CCF-1-foci obtain from mitochondria in young versus old animals (n=2 independent experiments with at least 40 animals/experiment; ****P<0.0001; two-tailed unpaired t-test). **D**, Representative image from Immunoblot analysis showing that CCF-1 is less associated with mitochondria in older animals compared to younger worms and **E**, Respective quantification of CCF-1 levels normalized to ATP-1 (n=3 independent experiments; *P<0.05; two-tailed unpaired t-test). Data information: Scale bars, 10μm. Images were acquired using a X63 objective lens. Error bars denote SEM.

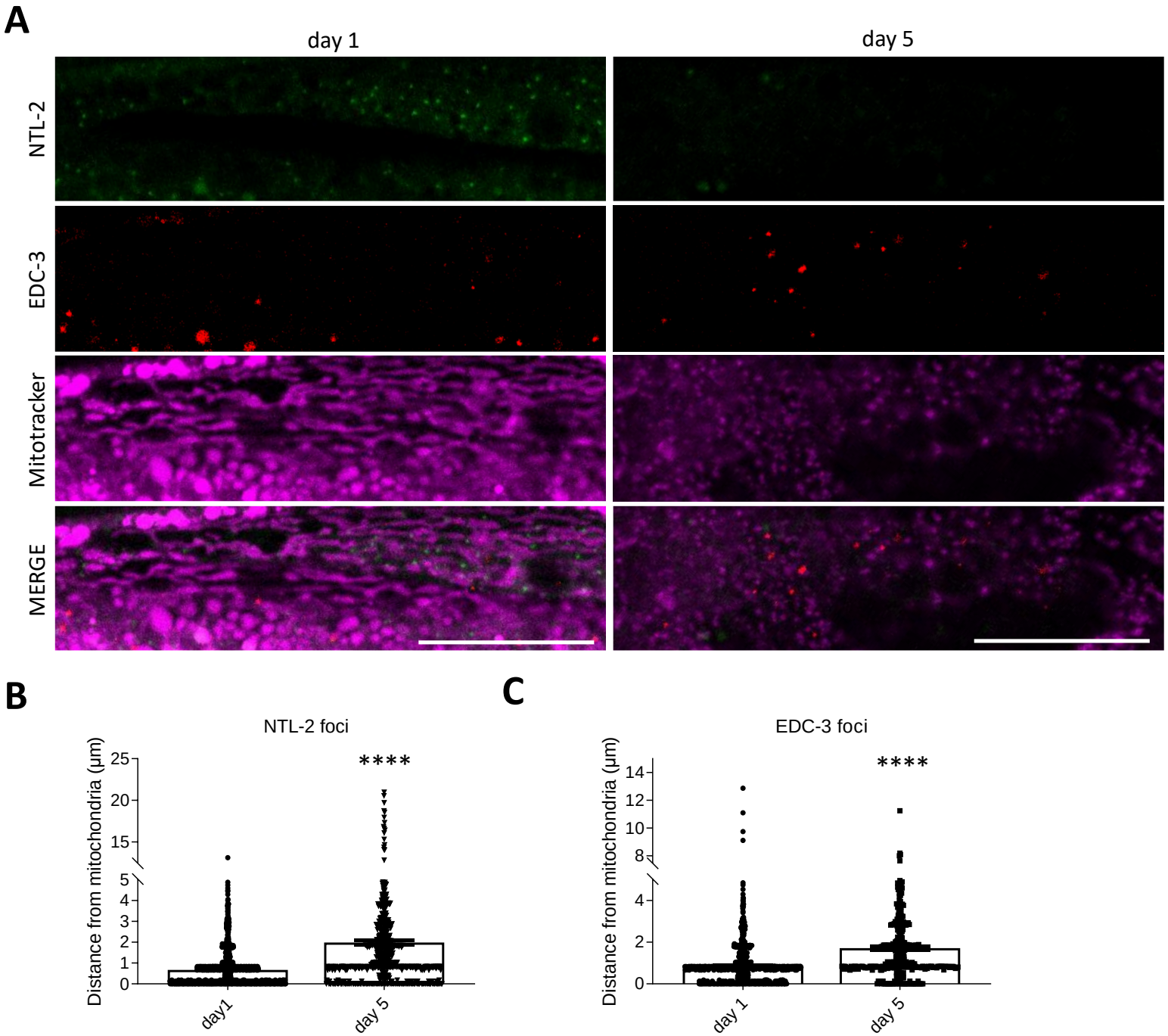

Appendix Fig S4

Appendix Figure S4 - NTL-2 and EDC-3 are coordinately associated with mitochondria in an age-dependent manner. Representative images showing the localization of NTL-2-foci and EDC-3-foci relative to mitochondria in **A**, young versus older animals (green: NTL-2, red: EDC-3, purple: Mitotracker Deep Red FM, a mitochondrial-specific dye). **B**, Quantification of the distances NTL-2- and **C**, EDC-3-foci obtain from mitochondria in young and older animals (n=3 independent experiments with at least 30 animals/experiment; ****P<0.0001; two-tailed unpaired t-test).

Data information: Scale bars, 20 µm. Images were acquired using a X63 objective lens. Error bars denote SEM.

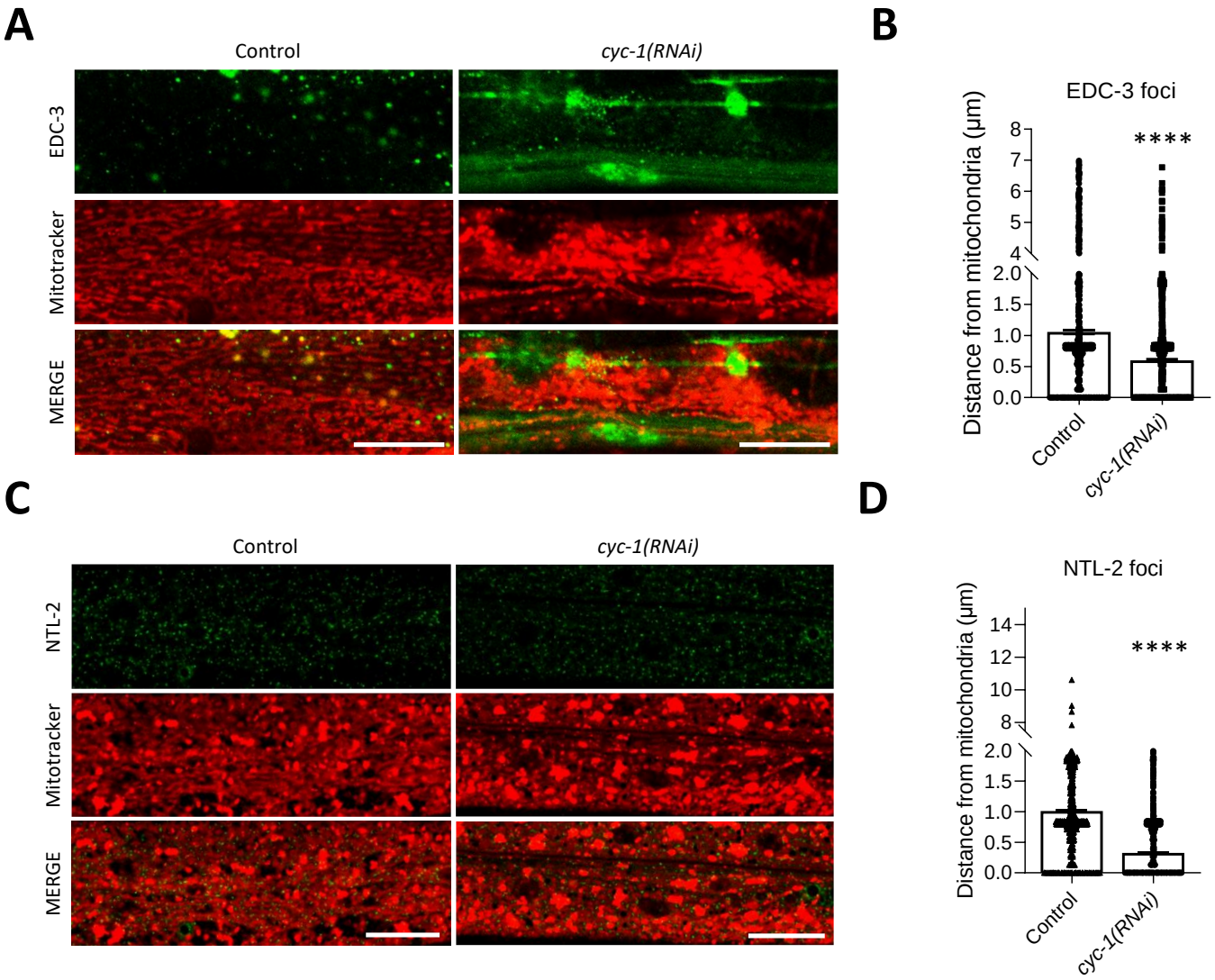

Appendix Fig S5

Appendix Figure S5 - NTL-2 and EDC-3 become tightly associated with mitochondria upon *cyc-1* genetic inhibition. A, Representative images showing the localization of EDC-3-foci relative to mitochondria upon genetic inhibition of *cyc-1* (green: EDC-3, red: Mitotracker Deep Red FM, a mitochondria-specific dye). **B**, Quantification of the distances between EDC-3-foci and mitochondria upon genetic inhibition of *cyc-1* (n=3 independent experiments with at least 30 animals/experiment; ****P<0.0001; unpaired two-tailed t test). **C**, Representative images showing the localization of NTL-2-foci relative to mitochondria upon genetic inhibition of *cyc-1* (green: NTL-2, red: Mitotracker Deep Red FM, a mitochondria-specific dye). **D**, Quantification of the distances between NTL-2-foci and mitochondria upon genetic inhibition of *cyc-1* (n=3 independent experiments with at least 30 animals/experiment; ****P<0.0001; two-tailed unpaired *t*-test).

Data information: Scale bars, 20 µm. Images were acquired using a X63 objective lens. Error bars denote SEM.

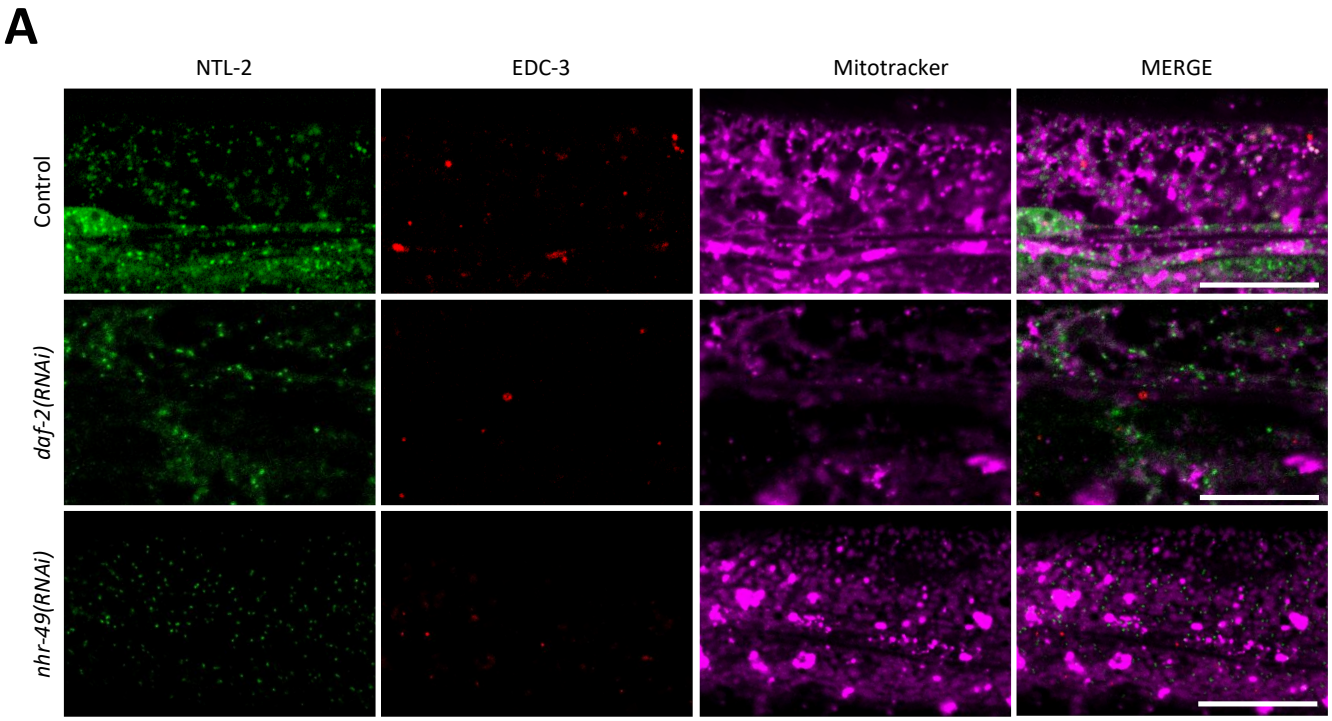

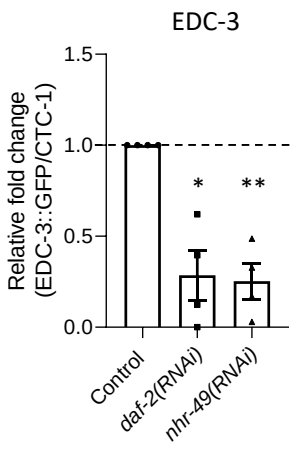

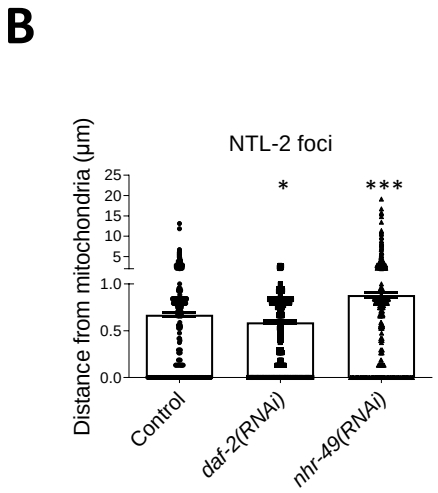

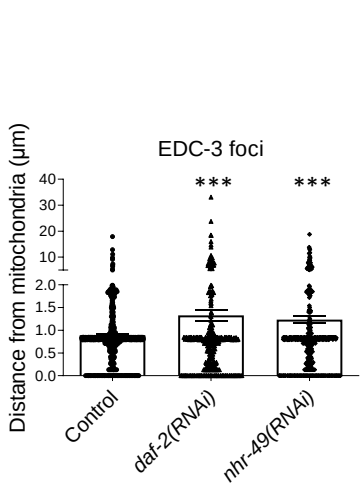

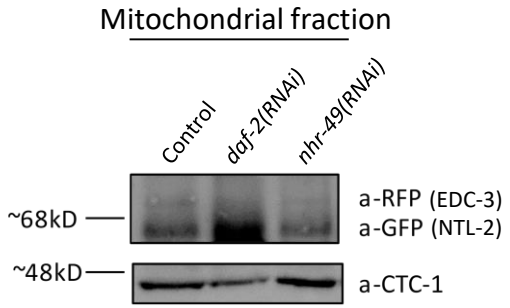

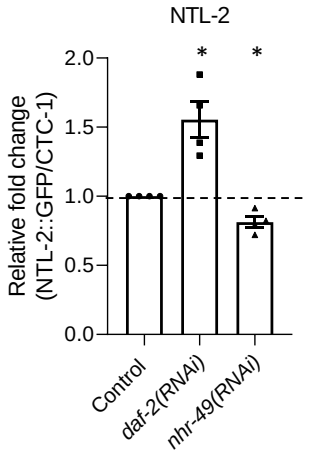

Appendix Fig S6

Appendix Figure S6 - Association of NTL-2- and EDC-3-foci with mitochondria in long- and short- lived animals deviates from their wild-type counterparts. A, Representative images showing the localization of NTL-2- and EDC-3-foci relative to mitochondria upon genetic inhibition of either *daf-2* or *nhr-49* (green: NTL-2, red: EDC-3, purple: Mitotracker Deep Red FM, a mitochondria-specific dye). **B**, Quantification of the distances NTL-2- and **C**, EDC-3-foci obtain from mitochondria upon genetic inhibition of either *daf-2* or *nhr-49* (n=3 independent experiments with at least 45 animals per experiment; *P<0.05, ***P<0.001; one-way analysis of variance (ANOVA)). **D**, Immunoblot analysis in isolated mitochondria of 1-day-old animals co-expressing EDC-3 and NTL-2. **E**, Quantification of EDC-3 and **F**, NTL-2 amount in the mitochondrial fraction obtained from animals subjected to the indicated genetic inhibitions compared to controls (n=4 independent experiments; *P<0.05, **P<0.01; Welch's one-way analysis of variance (ANOVA) followed by Dunnett's T3 multiple comparisons test). All experiments in this Figure have been performed in animals that co-express NTL-2 and EDC-3.

Data information: Scale bars, 20 μm. Images were acquired using a X63 objective lens. Error bars denote SEM.

A

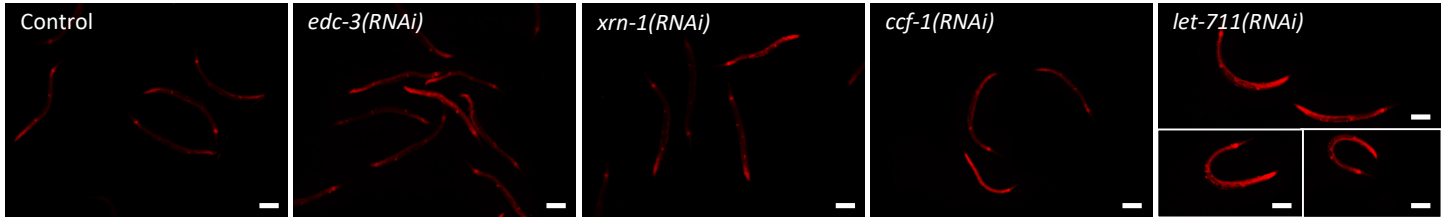

B

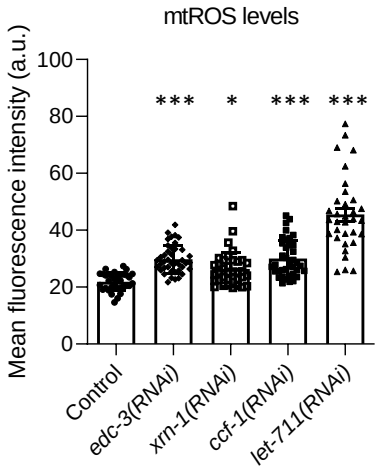

Appendix Fig S7

Appendix Figure S7 - Components of the CCR4-NOT and the mRNA degradation complexes alter mtROS production. A, Mitochondrial ROS production is elevated in animals subjected to *edc-3*, *xrn-1*, *ccf-1* or *let-711* RNAi and **B**, Respective quantification is shown (n=3 independent experiments with at least 182 animals/experiment; *P<0.05, ****P< 0.0001; one-way analysis of variance (ANOVA)).

Data information: Scale bars, 40μm. Images were acquired using a X5 objective lens. Error bars denote SEM.

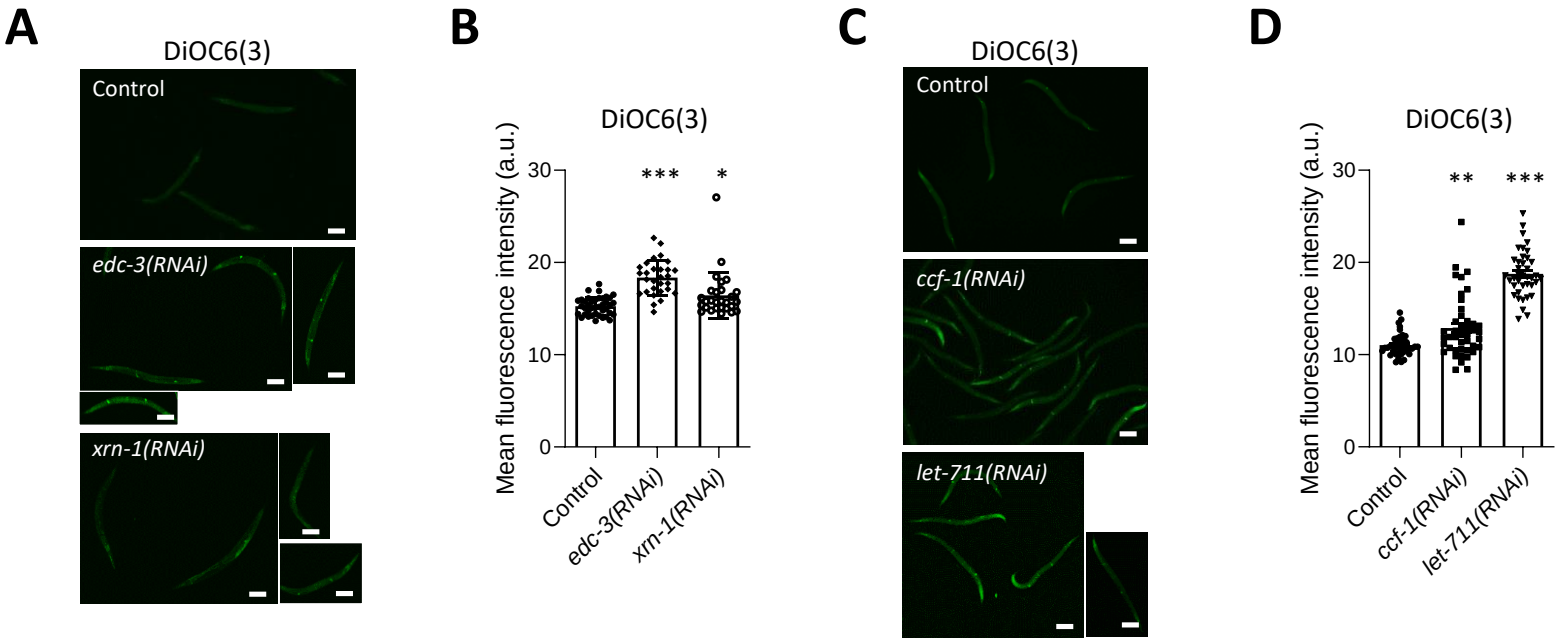

Appendix Fig S8

Appendix Figure S8 - Components of the CCR4-NOT and the mRNA degradation complexes alter mitochondrial membrane potential (Δψ). A, Representative images showing fluorescence intensity of the mitochondrial membrane potential dye DiOC6(3) in 1-day-old animals fed bacteria expressing control, *edc-3* or *xrn-1* RNAi and **B**, Respective quantification (n=3 independent experiments with at least 97 animals/experiment; *P< 0.05, ***P< 0.001; one-way analysis of variance (ANOVA)). **C**, Representative images showing fluorescence intensity of the mitochondrial membrane potential dye DiOC6(3) in 1-day-old animals fed bacteria expressing control, *ccf-1* or *let-711* RNAi and **D**, Respective quantification (n=3 independent experiments with at least 124 animals/experiment; **P< 0.01, ***P< 0.001; one-way analysis of variance (ANOVA)).

Data information: Scale bars, 40μm. Images were acquired using a X4 objective lens. Error bars denote SEM.

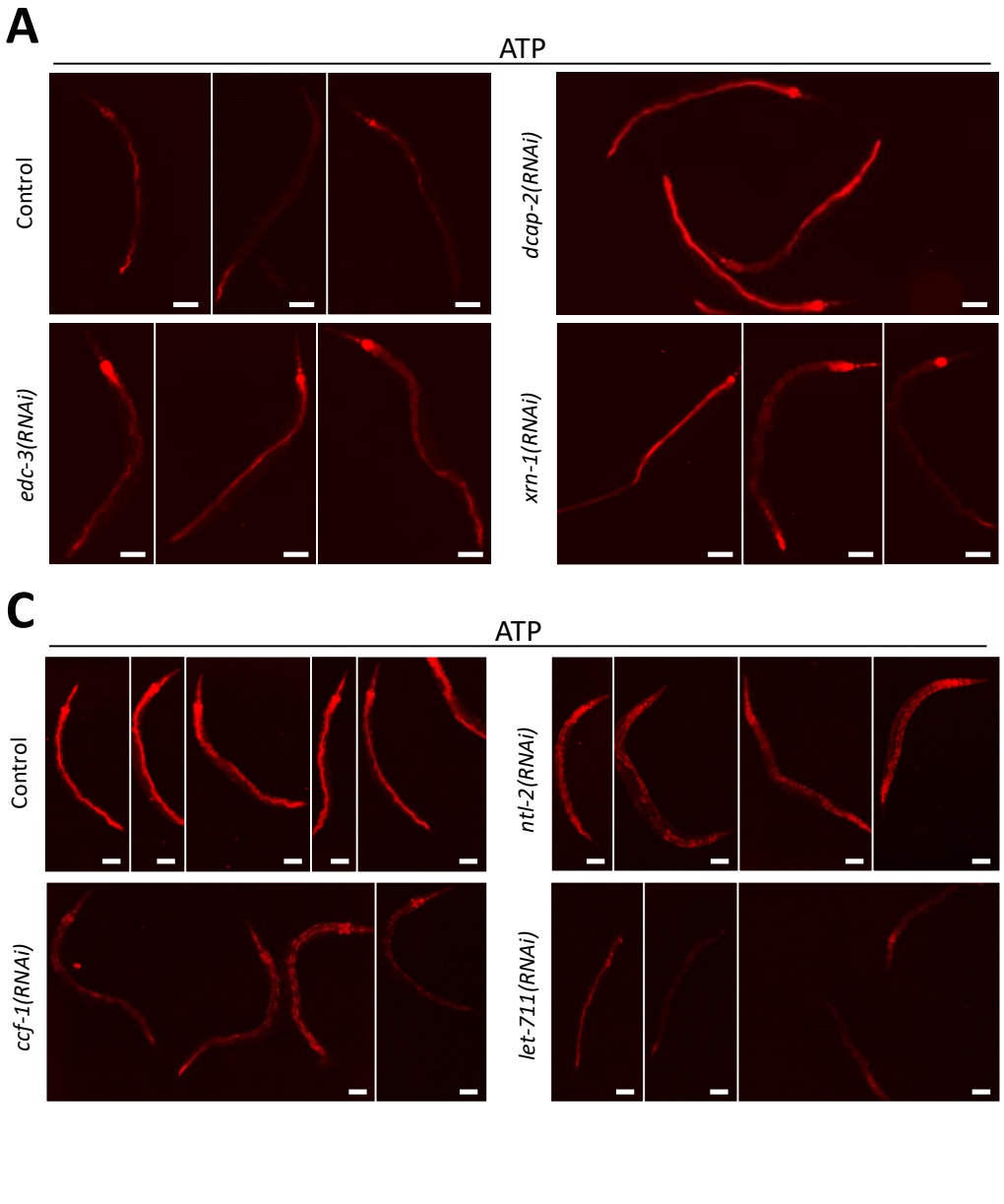

Appendix Fig S9

Appendix Figure S9 - Components of the CCR4-NOT and the mRNA degradation complexes alter mitochondrial ATP levels. A, Representative fluorescent images showing mitochondrial ATP levels in young adult animals fed with bacteria expressing control, *edc-3*, *dcap-2* and *xrn-1* RNAis. **B**, Corresponding quantification is shown (n=3 independent experiments with at least 120 animals/experiment; ***P< 0.001; one-way analysis of variance (ANOVA)). **C**, Representative fluorescent images showing mitochondrial ATP levels in young adult animals fed with bacteria expressing control, *ntl-2*, *ccf-1* and *let-711* RNAis. **D**, Corresponding quantification is shown (n=3 independent experiments with at least 130 animals/experiment; ***P< 0.001; one-way analysis of variance (ANOVA)). BioTracker ATP-Red was used for *in vivo* monitoring of mitochondrial ATP levels.

Data information: Scale bars, 20µm. Images were acquired using a X4 objective lens. Error bars denote SEM.

A

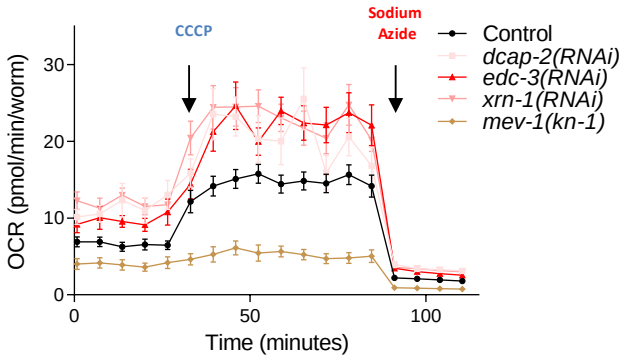

B

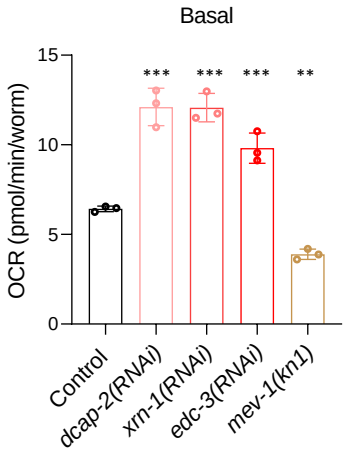

C

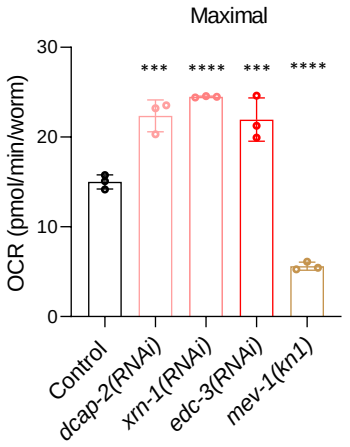

Appendix Fig S10

Appendix Figure S10 - Components of the mRNA degradation complex alter basal and maximal oxygen consumption rates (OCRs). A, Normalized OCRs profile plot versus time. **B**, Basal OCR per worm was measured at time points 3-5; before CCCP injection. **C**, Maximal OCR per worm was measured at time points 7-9 between CCCP and sodium azide injections. Seahorse XF analyzer was used to measure oxygen consumption rate (OCR) following a sequential injection of CCCP and sodium azide at the indicated time points. (n=2 independent experiments; **P< 0.01, ***P< 0.001, ****P<0.0001; one-way analysis of variance (ANOVA) followed by Dunnett's multiple comparison test).

Data information: Error bars denote SEM.

A

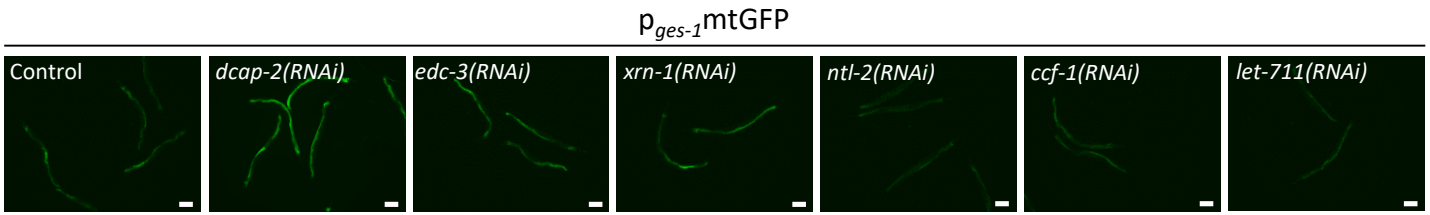

B

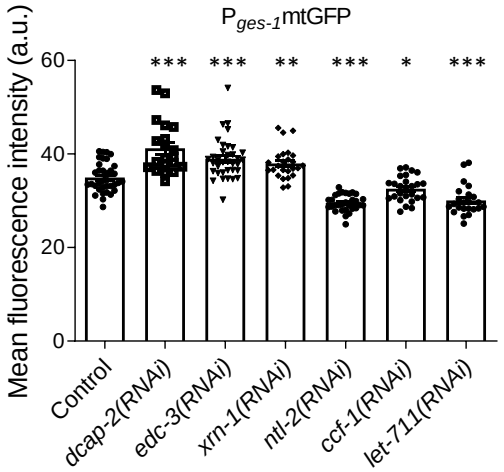

Appendix Fig S11

Appendix Figure S11 - Components of the CCR4-NOT and the mRNA degradation complexes alter intestinal mitochondrial abundance.

A, Representative images showing the effect of the indicated genetic inhibitions on the abundance of intestinal cell mitochondria in 1-day-old nematodes. **B**, Respective quantification is shown. (n=3 independent experiments with at least 194 animals/experiment; *P< 0.05, **P< 0.01, ***P< 0.001; one-way analysis of variance (ANOVA)).

Data information: Scale bars, 40µm. Images were acquired using a X4 objective lens. Error bars denote SEM.

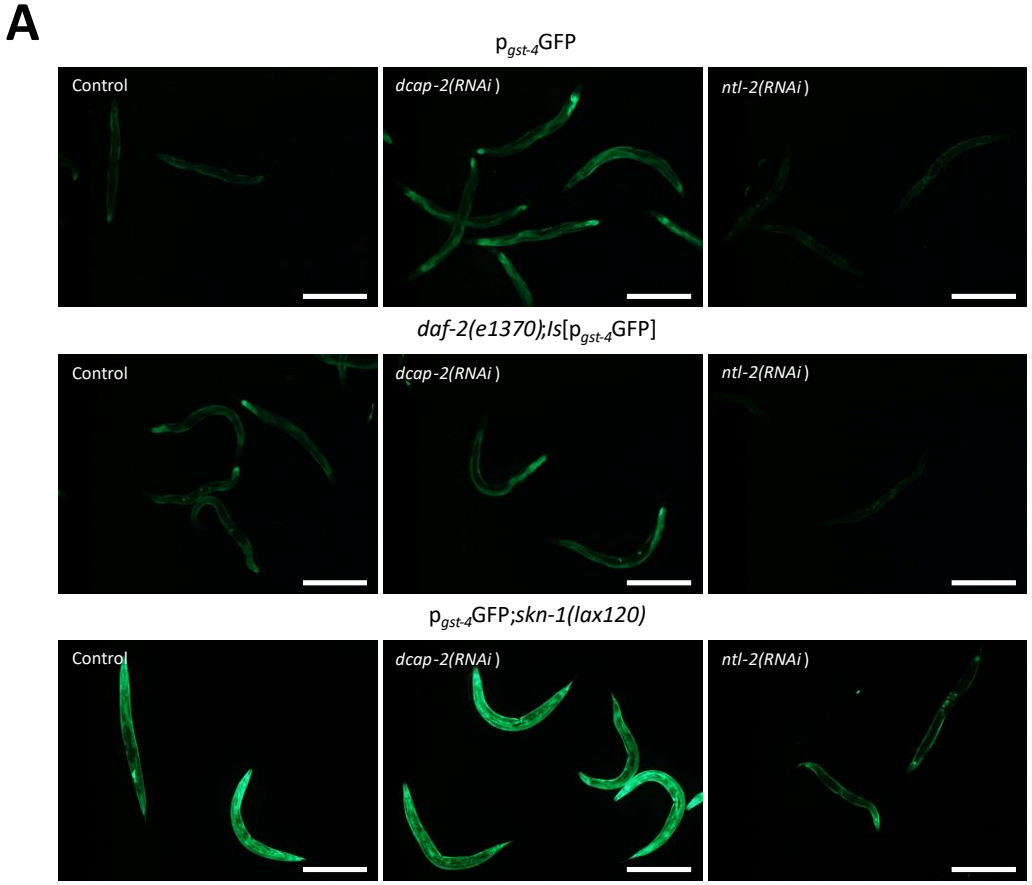

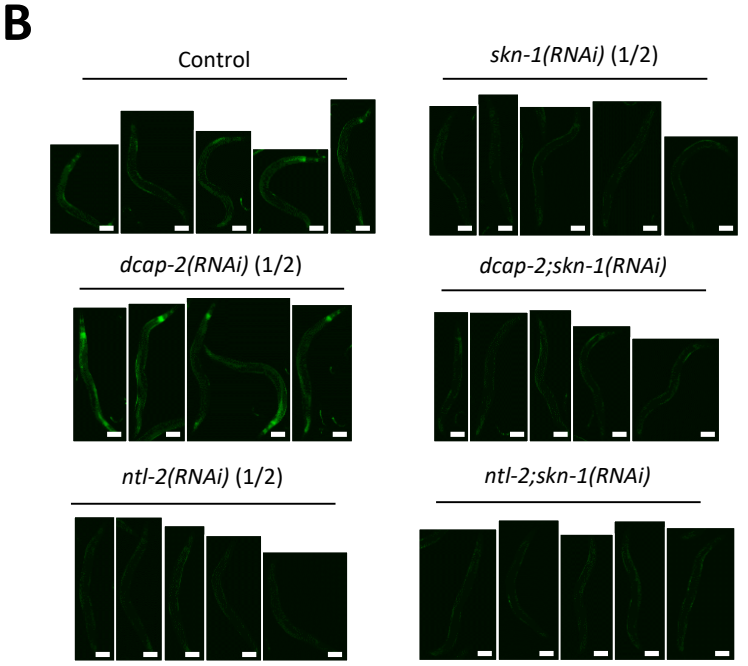

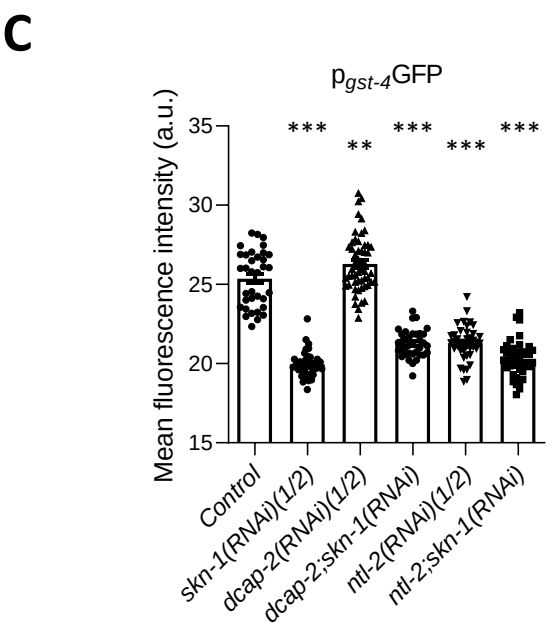

Appendix Fig S12

Appendix Figure S12 - Components of the CCR4-NOT and the mRNA degradation complexes alter *gst-4* promoter expression in a SKN-1-dependent manner. A, Representative images corresponding to quantification shown in Fig 3C, Scale bars, 50µm. Images were acquired using a X5 objective lens. **B**, Representative images showing the expression levels of p_{gst-4}GFP in 1-day-old animals upon the indicated RNAi treatments diluted 1:1 and **C**, Respective quantification (n=3 independent experiments with at least 244 animals/experiment; **P<0,01, ***P< 0.001; one-way analysis of variance (ANOVA)).

Data information: Scale bars, 20µm. Images were acquired using X5 and X4 objective lenses. Error bars denote SEM.

A

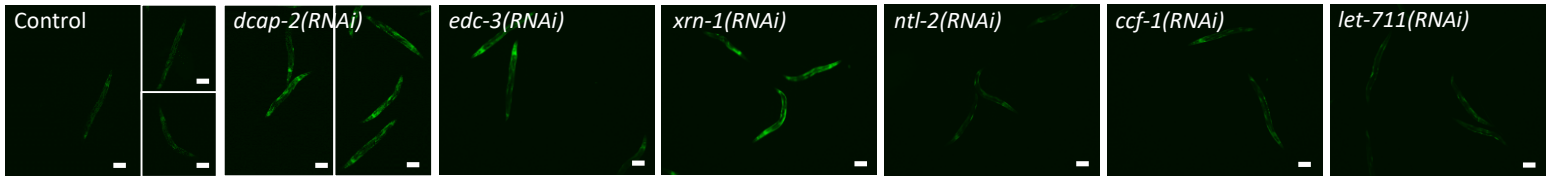

B

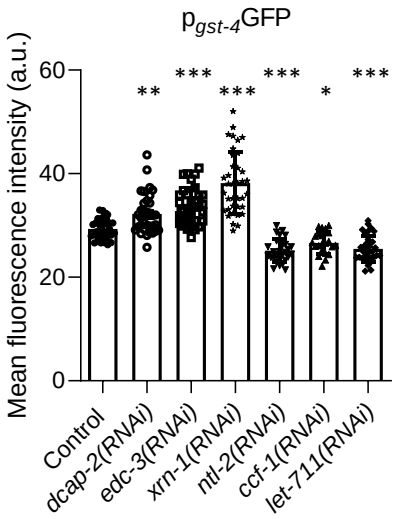

Appendix Fig S13

Appendix Figure S13 - Perturbation of the CCR4-NOT and the mRNA degradation complexes alters *gst-4* promoter expression. A, Measurement of the promoter activity of the SKN-1 target gene *gst-4* in 1-day-old animals upon the indicated RNAi treatments and **B**, Respective quantification is shown (n=3 independent experiments with at least 223 animals/experiment; **P<0,01, ***P< 0.001; one-way analysis of variance (ANOVA)).

Data information: Scale bars, 20µm. Images were acquired using a X4 objective lens. Error bars denote SEM.

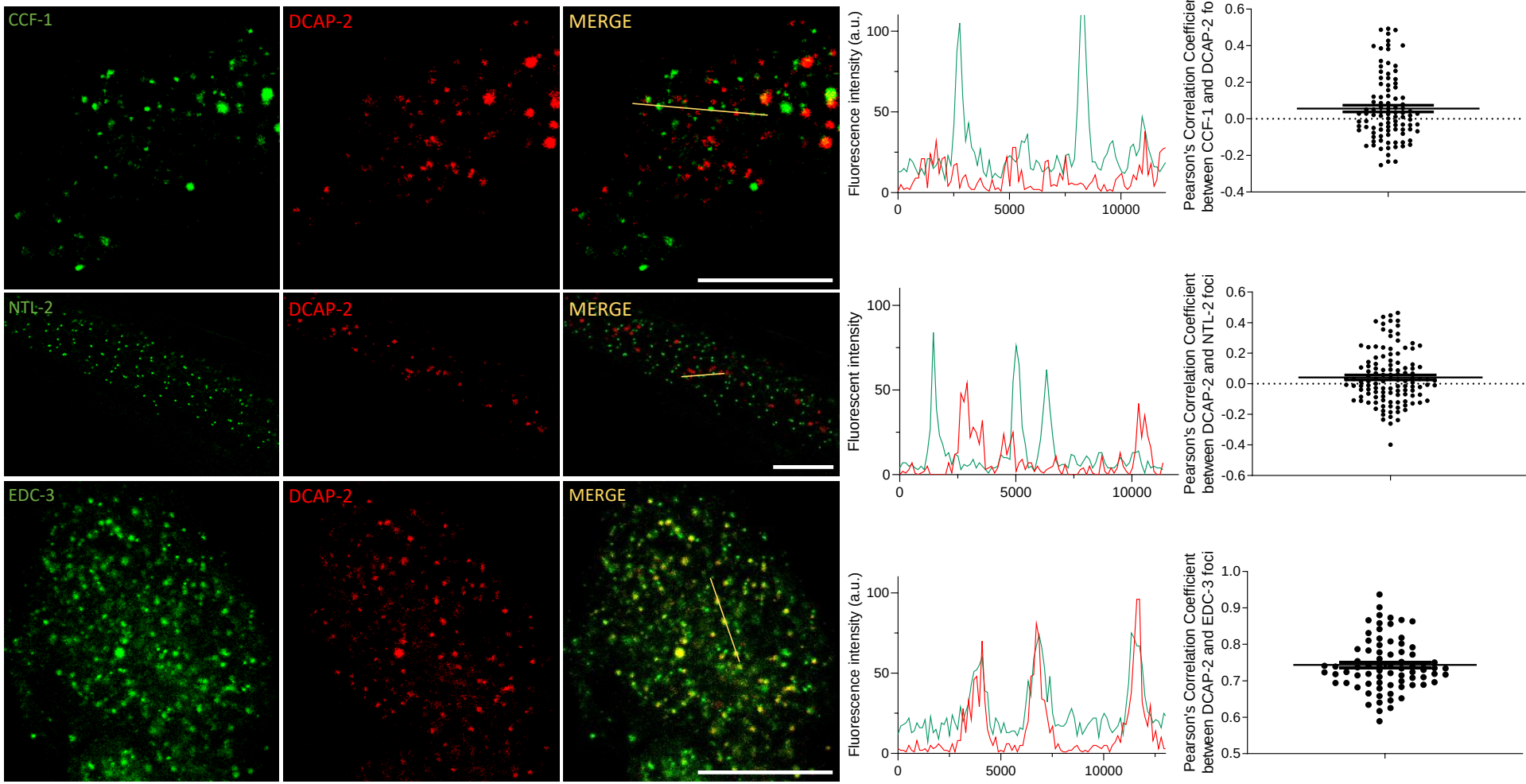

Appendix Fig S14

Appendix Figure S14 - Components of the CCR4-NOT and the mRNA degradation complexes localize in distinct foci. A, (top) Representative images showing the localization of CCF-1- (green) and DCAP-2- (red) foci in transgenic animals that co-express them, (middle) representative images showing the localization of NTL-2- (green) and DCAP-2- (red) labeled foci in transgenic animals that co-express them and (bottom) representative images showing the localization of EDC-3- (green) and DCAP-2- (red) labeled foci in transgenic animals that co-express them. **B**, Respective fluorescent intensity graphs of the foci marked with the yellow line in panel A. **C**, (top) Pearson's correlation coefficient values after measuring the correlation between CCF-1- and DCAP-2-foci, (middle) Pearson's correlation coefficient values after measuring the correlation between DCAP-2- and NTL-2-foci and (bottom) Pearson's correlation coefficient values after measuring the correlation between DCAP-2- and EDC-3-foci. (n=2 independent experiments with at least 15 animals for each strain/experiment).

Data information: Scale bar, 20μm. Images were acquired using the X63 lens. Error bars denote SEM.

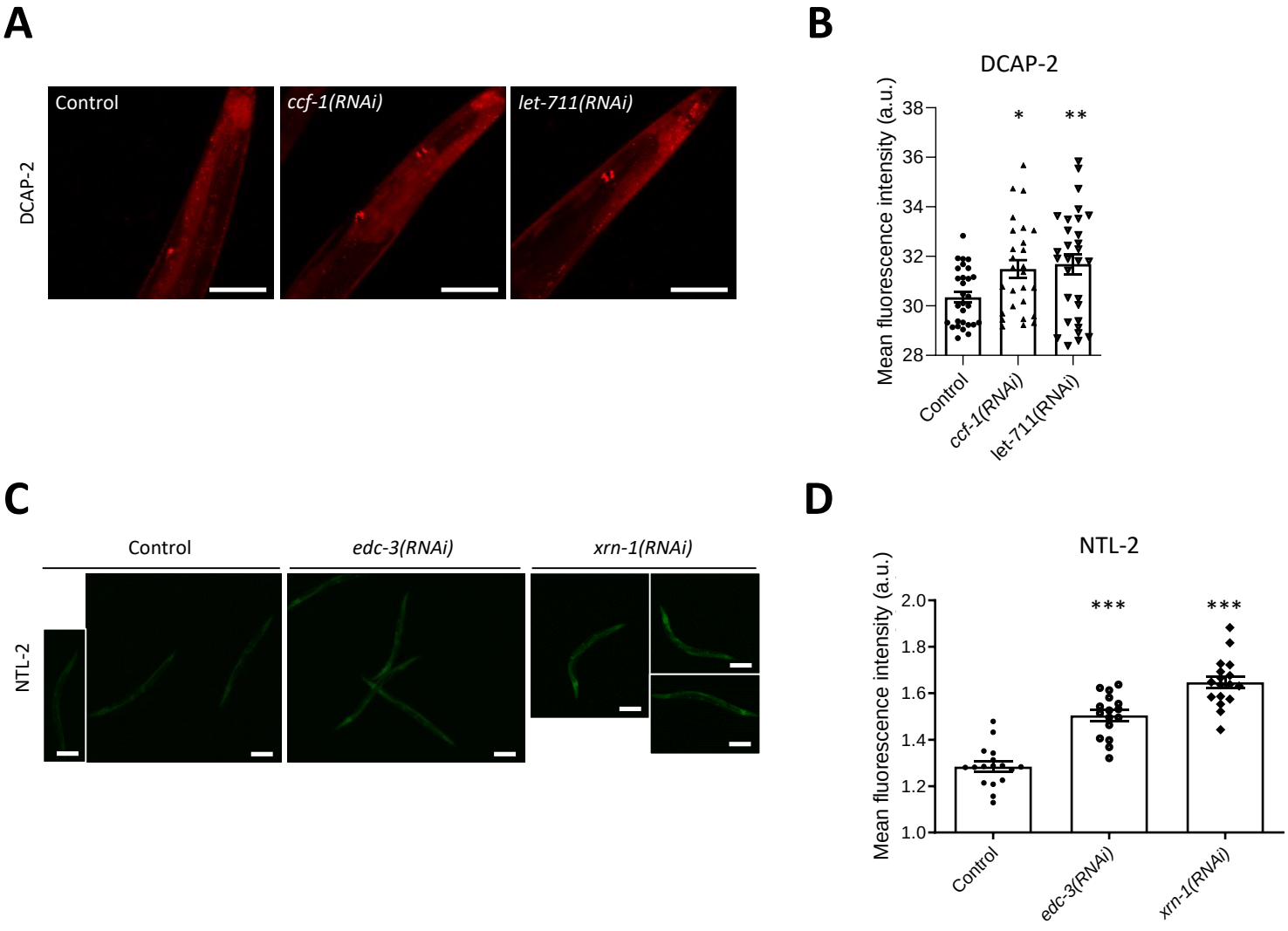

Appendix Fig S15

Appendix Figure S15 - Genetic inhibition of the one type of body triggers an elevation in the protein abundance of components of the other type. A, Representative images showing DCAP-2 expression in the posterior half of young adult animals upon genetic inhibition of storage body components. Scale bar, 100μm. Images were acquired using the X40 lens. **B**, Quantification of DCAP-2 levels in whole animals (n=3 independent experiments with at least 86 animals/experiment; *P< 0.05, **P< 0.01, one-way analysis of variance (ANOVA)). **C**, Representative images showing NTL-2 levels in young adult animals upon genetic inhibition of degradation body components and **D**, Respective quantification is shown (n=3 independent experiments with at least 50 animals/experiment; ***P< 0.001; one-way analysis of variance (ANOVA)).

Data information: Scale bar, 40μm. Images were acquired using the X4 lens. Error bars denote SEM.

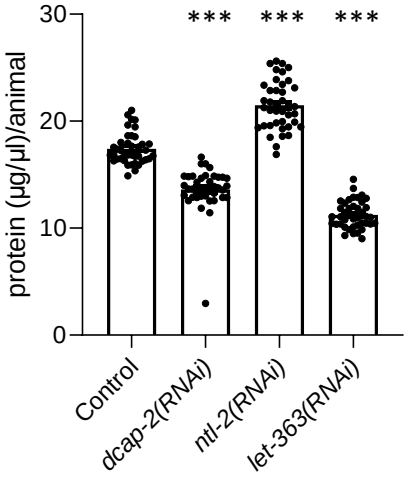

Appendix Fig S16

Appendix Figure S16 - Quantification of total protein content in 1-day-old whole worm lysates under control conditions and upon inhibition of the indicated genes. (n=3 independent experiments with at least 400 animals/experiment; ***P<0.001; one-way analysis of variance (ANOVA)).

Data information: Error bars denote SEM.

A

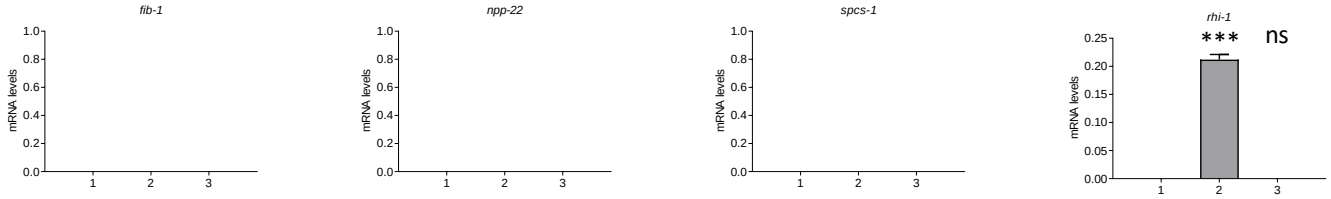

1: *unc-119(ed3)III;Ex*[$p_{ntl\text{-}2}$NTL-2::GFP;UNC-119(+)]

2: p_{gst4}GFP

3: *unc-119(ed3)III*

B

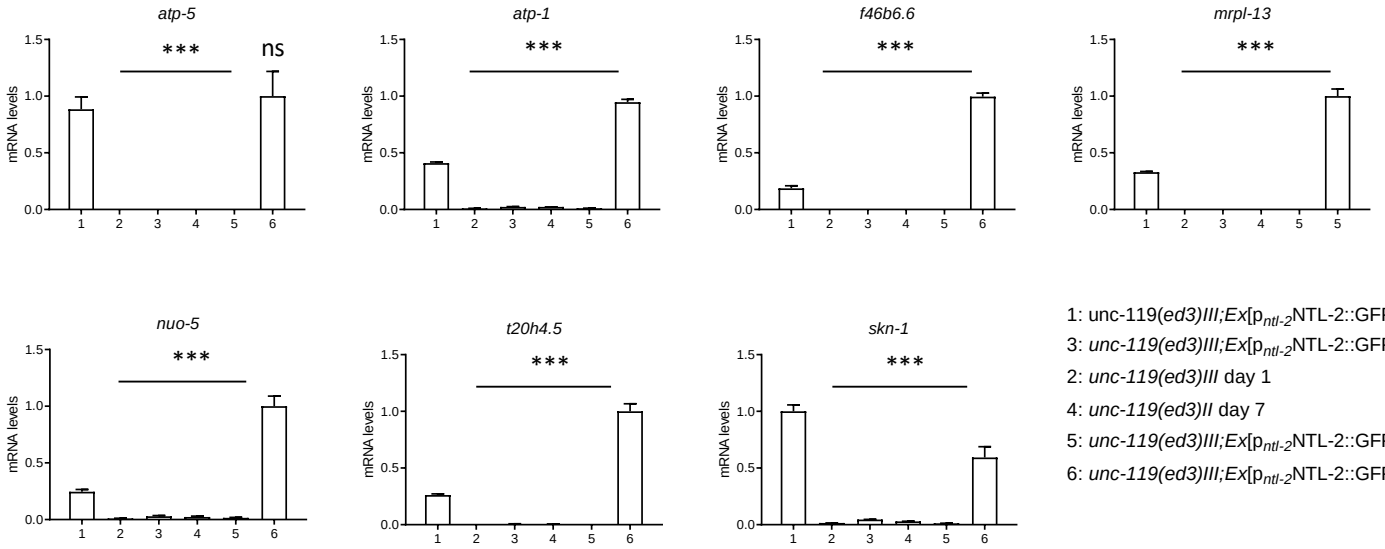

1: unc-119(*ed3)III;Ex*[$p_{ntl\text{-}2}$NTL-2::GFP;UNC-119(+)] day 1

3: *unc-119(ed3)III;Ex*[$p_{ntl\text{-}2}$NTL-2::GFP;UNC-119(+)] day 7

2: *unc-119(ed3)III* day 1

4: *unc-119(ed3)II* day 7

5: *unc-119(ed3)III;Ex*[$p_{ntl\text{-}2}$NTL-2::GFP;UNC-119(+)] day1+CCCP

6: *unc-119(ed3)III;Ex*[$p_{ntl\text{-}2}$NTL-2::GFP;UNC-119(+)] day 1+ *dcap-2(RNAi)*

Appendix Fig S17

Appendix Figure S17 - NTL-2 preferentially binds MTPTs and their association is affected by age, mitochondrial stress and genetic inhibition of *dcap-2*. A, Analysis of expression of mRNAs encoding nuclear (FIB-1, NPP-22), ER (SPCS-1) and cytoplasmic (RHI-1) proteins by real time quantitative RT-PCR following RNA immunoprecipitation (RIP) in anti-GFP isolates from NTL-2::GFP transgenic animals, *unc-119(ed3)III* and p_{gst-4}GFP counterparts (used as negative controls) (n=2 independent experiments; ***P< 0.001; one-way analysis of variance (ANOVA)). **B**, Analysis of expression of select MTPTs by real time quantitative RT-PCR following RNA immunoprecipitation (RIP) in anti-GFP isolates from NTL-2::GFP transgenic and *unc-119(ed3)III* animals during ageing, upon CCCP treatment and genetic inhibition of *dcap-2* (n=2 independent experiments; ***P< 0.001; one-way analysis of variance (ANOVA)).

Data information: Error bars denote SEM. Numbers at the x axis represent sample names described after the last bar plot in the right part of each figure panel.

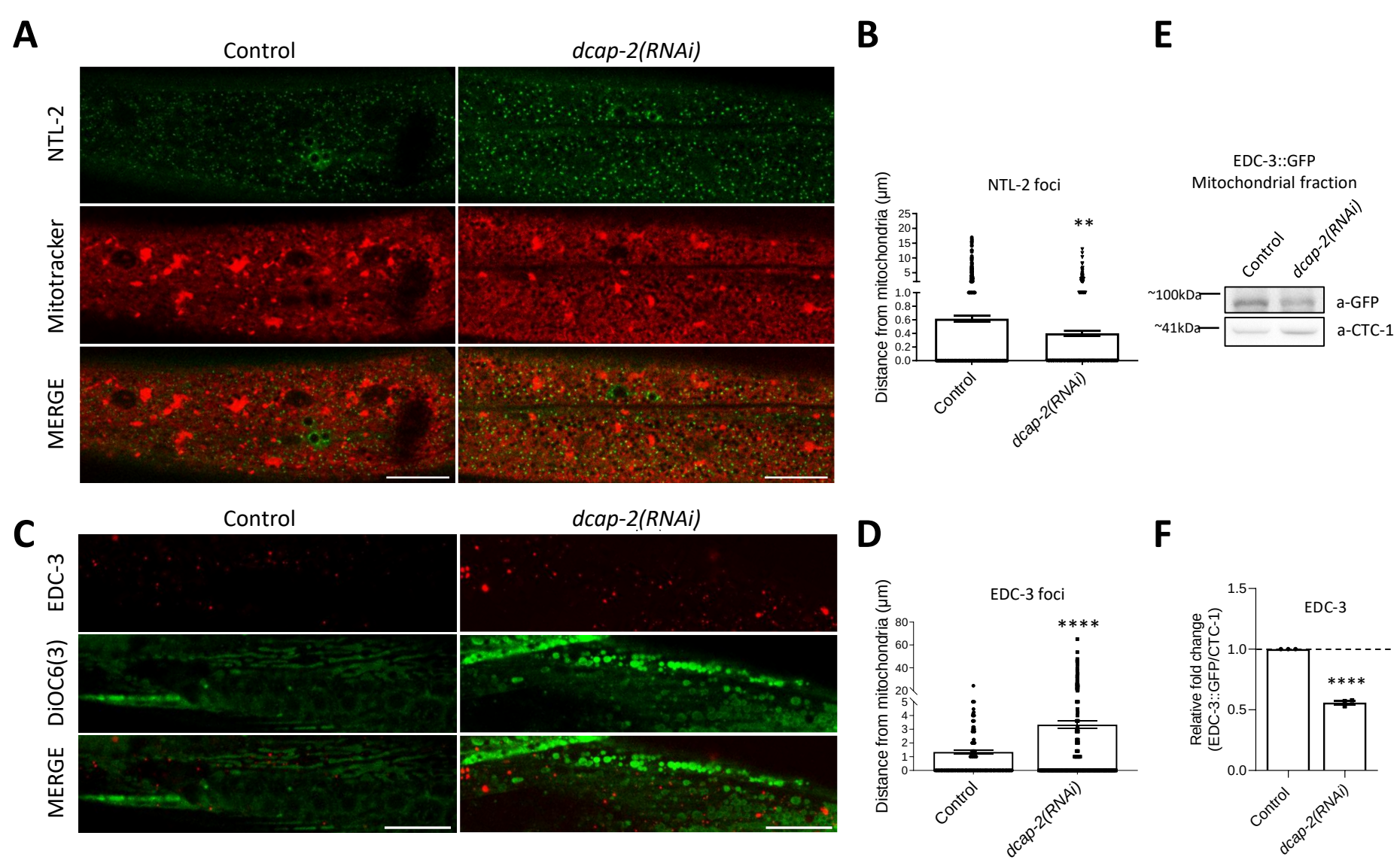

Appendix Fig S18

Appendix Figure S18 - Association of storage and degradation bodies with mitochondria is oppositely affected by genetic inhibition of *dcap-2.* **A**, Representative images showing the localization of NTL-2/storage bodies relative to mitochondria upon genetic inhibition of *dcap-2* (green: NTL-2, red: Mitotracker Deep Red FM, a mitochondrial specific dye). **B**, Quantification of the distances between NTL-2/storage bodies and mitochondria upon genetic inhibition of *dcap-2* (n=3 independent experiments with at least 30 animals/experiment; **P<0.01; two-tailed unpaired *t*-test). **C**, Representative images showing the localization of EDC-3/degradation bodies relative to mitochondria upon genetic inhibition of *dcap-2* (red: EDC-3, green: DiOC6(3), a mitochondria-specific dye). **D**, Quantification of the distances between EDC-3/degradation bodies and mitochondria upon genetic inhibition of *dcap-2* (n=3 independent experiments with at least 30 animals per experiment; ****P<0.0001; two-tailed unpaired *t*-test). **E**, Representative image from Immunoblot analysis showing that EDC-3 is less associated with mitochondria upon genetic inhibition of *dcap-2* and **F**, Respective quantification of EDC-3 levels normalized to CTC-1 is shown (n= 3 independent experiments; ****P<0.0001; two-tailed unpaired *t*-test).

Data information: Scale bar, 20μm. Images were acquired using the X63 lens. Error bars denote SEM.

A

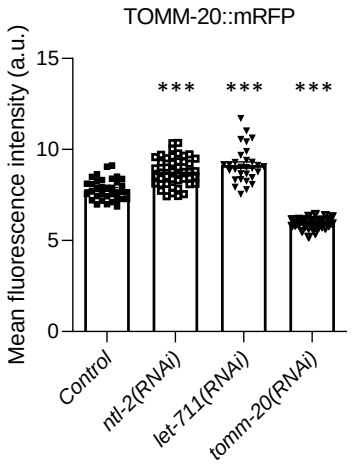

B

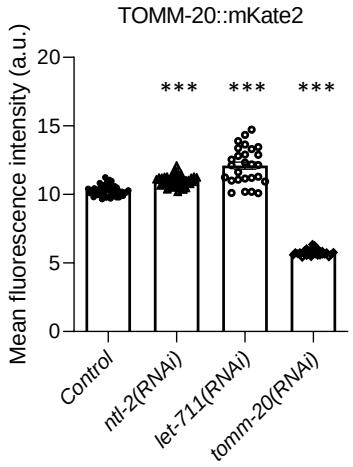

Appendix Fig S19

Appendix Figure S19 - TOMM-20 levels increase upon genetic inhibition of storage body components. A, Genetic inhibition of either *ntl-2* or *let-711* increases the expression levels of TOMM-20::mRFP expressed in body wall muscle cells. **B**, Genetic inhibition of either *ntl-2* or *let-711* increases the expression levels of TOMM-20::mKate2 ubiquitously expressed in all animal tissues. *tomm-20(RNAi)* is used as a control. (n=2 independent experiments with at least 141 animals/experiment (for A) and 147 animals/experiment (for B); ***P< 0.001; one-way analysis of variance (ANOVA)).

Data information: Error bars denote SEM.

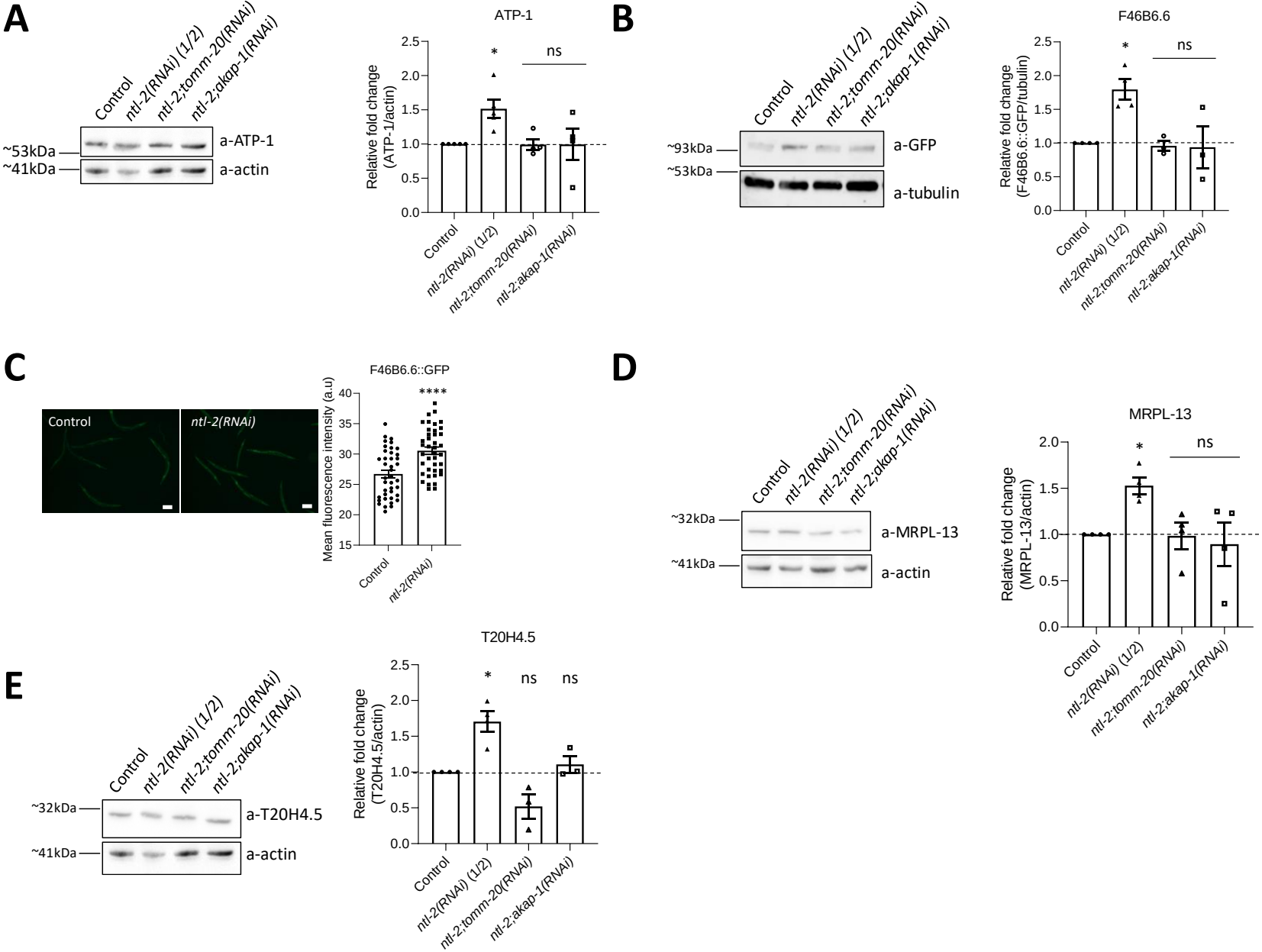

Appendix Fig S20

Appendix Figure S20 - Knockdown of *ntl-2* increases MTPT protein levels in a TOMM-20- and AKAP-1-dependent manner. A, (left) Immunoblot analysis in 1-day-old whole animal extracts showing the protein levels of ATP-1 in control conditions and upon the indicated genetic inhibitions and (right) respective quantification (n= at least 3 independent experiments; *P<0.05; one-way analysis of variance (ANOVA) followed by Dunnett's T3 multiple comparisons test). **B**, (left) Immunoblot analysis in 1-day-old whole animal extracts showing the protein levels of F46B6.6 in control conditions and upon the indicated genetic inhibitions and (right) respective quantification (n= at least 3 independent experiments; *P<0.05; one-way analysis of variance (ANOVA) followed by Dunnett's T3 multiple comparisons test). **C**, (left) Representative images showing F46B6.6 protein levels in 1-day-old animals fed bacteria expressing control or *ntl-2* RNAi. Scale bars, 40μm; and respective quantification is shown in right (n=2 independent experiments with at least 40 animals/experiment; ****P< 0.05; two-tailed unpaired *t*-test). **D**, (left) Immunoblot analysis in 1-day-old whole animal extracts showing the protein levels of MRPL-13 in control conditions and upon the indicated genetic inhibitions and respective quantification is shown in right (n= 4 independent experiments; *P<0.05; Welch's one-way analysis of variance (ANOVA) followed by Dunnett's T3 multiple comparisons test). **E**, (left) Immunoblot analysis in 1-day-old whole animal extracts showing the protein levels of T20H4.5 in control conditions and upon the indicated genetic inhibitions (n= at least 3 independent experiments; *P<0.05; Welch's one-way analysis of variance (ANOVA) followed by Dunnett's T3 multiple comparisons test).

Data information: Error bars denote SEM.

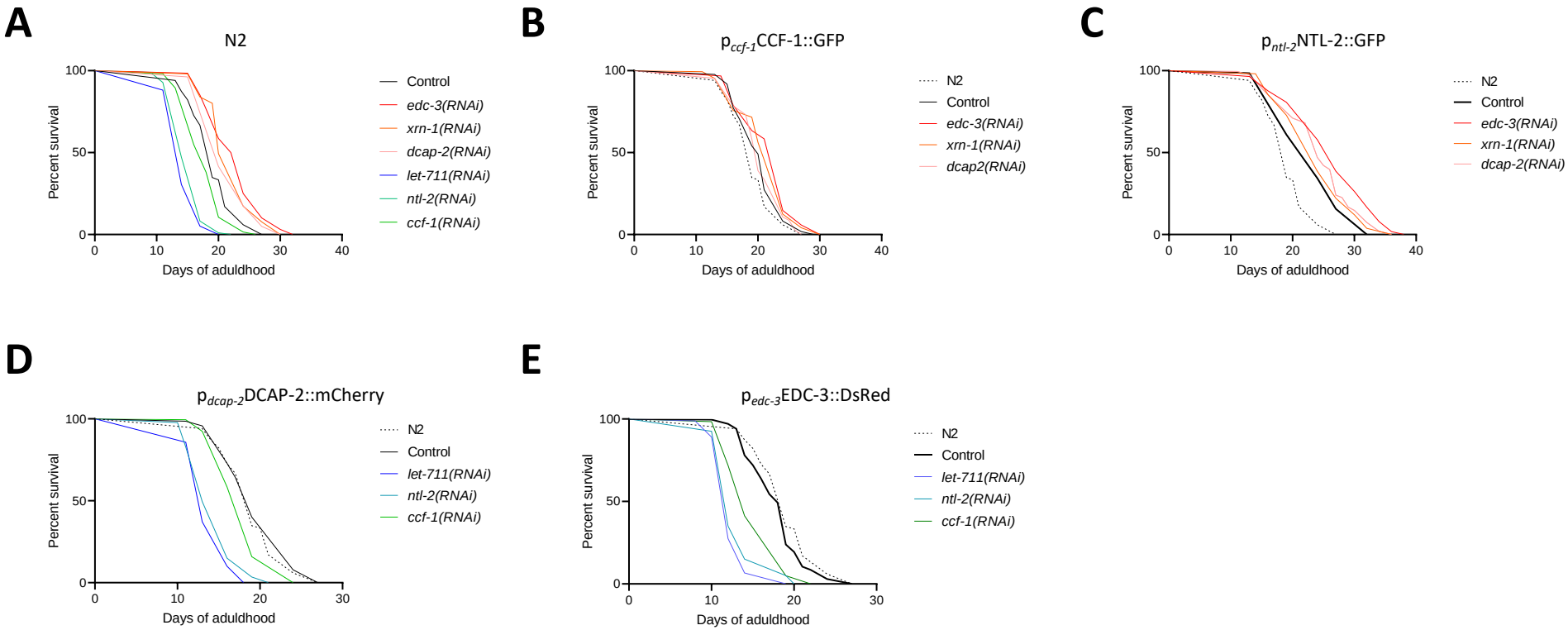

Appendix Fig S21

Appendix Figure S21 - Balance of storage and degradation body components regulates lifespan. A, Knockdown of storage and degradation body components oppositely affect longevity. **B**, Knockdown of degradation body components further extends the lifespan of CCF-1 overexpressing animals. **C**, Knockdown of degradation body components extends the lifespan of NTL-2 overexpressing animals. **D**, Knockdown of storage body components shortens the lifespan of transgenic animals overexpressing DCAP-2. **E**, Knockdown of storage body components shortens the lifespan of transgenic animals overexpressing EDC-3.

Data information: Lifespan assays were performed at 20ºC; detailed lifespan data are given in Table EV4.

A

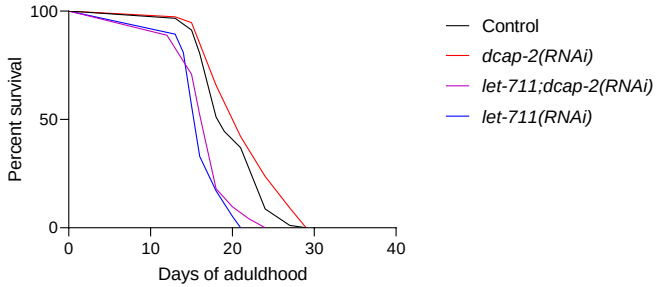

B

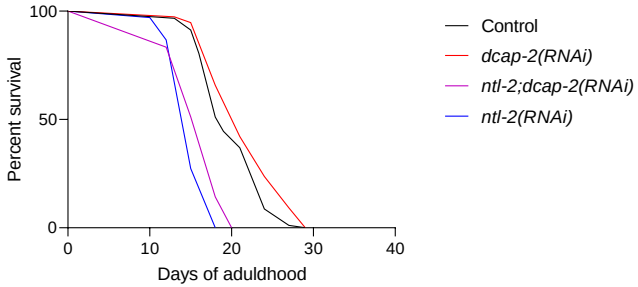

C

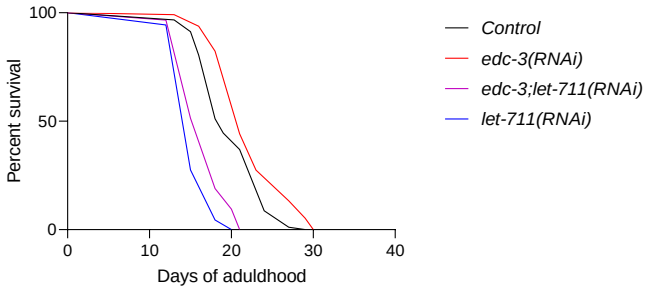

D

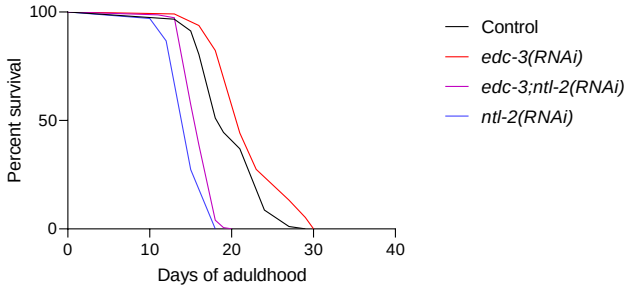

E

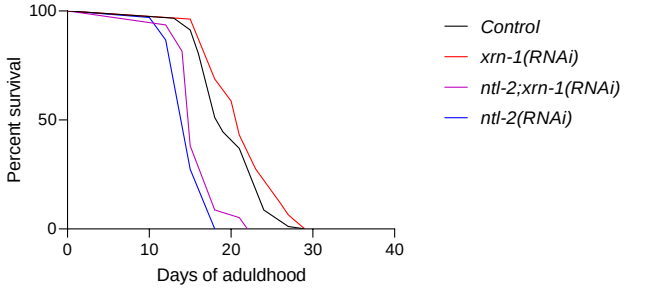

Appendix Fig S22

Appendix Figure S22 - Effects of concomitant knockdown of storage and degradation body components on longevity. A, Concomitant knockdown of *let-711* and *dcap-2* reverses *dcap-2* longevity. **B**, Concomitant knockdown of *ntl-2* and *dcap-2* reverses *dcap-2* longevity. **C**, Concomitant knockdown of *edc-3* and *let-711* reverses *edc-3* longevity. **D**, Concomitant knockdown of *edc-3* and *ntl-2* reverses *edc-3* longevity. **E**, Concomitant knockdown of *ntl-2* and *xrn-1* reverses *xrn-1* longevity.

Data information: Lifespan assays were performed at 20ºC; detailed lifespan data are given in Table EV4.

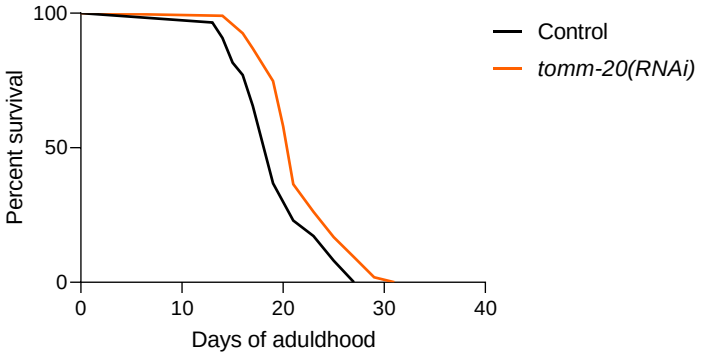

Appendix Fig S23

Appendix Figure S23 - *tomm-20* knockdown extends lifespan.

Data information: Lifespan assays were performed at 20^{o}C; detailed lifespan data are given in Table EV4.